https://doi.org/10.23960/jvs.v2i1.0037

INSTEP PUB

JURNAL SAINTEK DAN VOKASI

E-ISSN | P-ISSN

Volume 2 Edisi 1, Mei 2026

JVS

Synthesis and Characterization of Natural Source-Based Hydroxyapatite Composites for Bone Implant Applications: A Comprehensive Review

Syaipudin Anwar[1], , Nindya Indah Kusumawardani[2,*]

[1] *Departement of Mechanical Engineering, Universitas Lampung, Jl. Prof. Soemantri Brojonegoro, Bandar Lampung 35145*
[2]*Department of Chemical Engineering, Universitas Lampung, Jl. Prof. Soemantri Brojonegoro, Bandar Lampung 35145*

INFORMASI ARTIKEL

Article history
Received : 01-05-2026
Revised : 23-05-2026
Accepted : 28-05-2026

Kata kunci:
Hydroxyapatite;
Natural precursors;
Biocompatibility;
Tissue engineering;
Composite.

ABSTRAK

Hydroxyapatite (HAp, $Ca_{10}(PO_4)_6(OH)_2$) is the principal inorganic component of human bone and has been extensively investigated as a biomaterial for bone implants, scaffolds, and coatings. The conventional synthesis of HAp from analytical-grade chemical reagents is associated with high production costs and limited sustainability. In recent years, natural and bio-waste sources including eggshells, chicken bones, fish bones, bovine bones, seashells, and geological limestone ($CaCO_3$) have attracted significant research attention as cost-effective and environmentally sustainable precursors for HAp synthesis. This comprehensive review critically examines advances in: (i) synthesis methodologies (wet precipitation, sol-gel, hydrothermal, calcination, and microwave-assisted routes); (ii) characterization techniques (XRD, FTIR, SEM-EDS, TEM, BET, and mechanical testing); (iii) composite development combining natural HAp with biopolymers (chitosan, collagen, PLGA) and metals (titanium, zinc); and (iv) biological performance encompassing in vitro biocompatibility, in vivo osseointegration, and simulated body fluid (SBF) bioactivity testing. Special focus is given to the conversion of geological limestone ($CaCO_3$) and chicken bone into phase-pure HAp, the influence of processing parameters on crystallinity and Ca/P ratio, and the mechanical and biological performance of the resulting composites for bone implant applications. Analysis of 78 peer-reviewed publications confirms that naturally derived HAp exhibits Ca/P ratios of 1.65–1.67, high biocompatibility (cell viability >90%), and superior or comparable bioactivity relative to synthetic counterparts, establishing a strong foundation for next-generation sustainable orthopedic and dental biomaterials.

1. Introduction

Bone defects arising from trauma, tumor resection, congenital abnormalities, and degenerative diseases represent a leading cause of disability worldwide, with an estimated 2.2 million bone grafting procedures performed annually [1]. Current clinical strategies encompass autografts (gold standard), allografts, and synthetic implants; however, autograft harvesting inflicts donor-site morbidity, and allografts carry risks of immune rejection and pathogen transmission [2]. These limitations have accelerated intensive research into synthetic biomaterials that replicate the hierarchical structure and biological function of natural bone.

Hydroxyapatite (HAp, $Ca_{10}(PO_4)_6(OH)_2$), the dominant mineral phase of human bone and teeth, is the most extensively investigated bioceramic for bone repair applications. Its chemical composition closely mimics the inorganic component of bone (~70 wt% mineral, Ca/P molar ratio = 1.67), endowing it with outstanding biocompatibility, osteoconductive properties, and direct bonding capacity to living bone tissue without eliciting a toxic or immunogenic response [1],[2],[3]. HAp has been successfully employed in clinical forms including bone graft substitutes, porous scaffolds for tissue engineering, coatings on metallic implants, and drug delivery systems [3].
Conventional HAp synthesis relies on high-purity chemical precursors such as $Ca(OH)_2$ and H_3PO_4 or diammonium hydrogen phosphate, incurring significant raw material costs

*Email korespondensi: nindya.indahwardani@eng.unila.ac.id

and generating chemical waste. In response, a growing body of literature has focused on deriving HAp from bio-waste and geological natural sources rich in calcium carbonate ($CaCO_3$) or calcium phosphate, including eggshells [5],[14],[15], chicken bones [17],[18],[21], fish bones [4],[11], bovine bones [22],[23], seashells [31],[32], and geological limestone [27],[28],[29],[30]. These precursors offer multiple advantages: global abundance, low acquisition cost, reduced chemical waste, and retention of trace mineral elements (Mg^{2+}, Sr^{2+}, Zn^{2+}, Na^{+}) that may enhance the biological performance of the synthesized HAp [26].

Among natural calcium precursors, geological limestone (predominantly calcite $CaCO_3$) is particularly noteworthy for large-scale HAp production, given its widespread geological availability and established industrial processing infrastructure [27],[29],[30]. Chicken bone, with an inorganic phase of approximately 65% calcium phosphate apatite, represents the simplest direct route to HAp via thermal calcination, yielding a material that retains biological trace elements characteristic of skeletal mineral [17],[18],[21]. Both precursors have been demonstrated to yield phase-pure, stoichiometric HAp with Ca/P ratios approaching 1.67 and comparable bioactivity to synthetic HAp [28],[30].

Despite significant advances, challenges remain in ensuring batch-to-batch consistency from variable natural sources, overcoming the inherent mechanical brittleness of monolithic HAp for load-bearing applications, and navigating the regulatory pathway for clinical translation. Composite strategies combining naturally derived HAp with biopolymers (chitosan, collagen, PLGA) and metallic phases (titanium, zinc) address the mechanical limitations while preserving or enhancing biological performance [42],[45],[47].

This article presents a comprehensive and critical review of the state-of-the-art in the synthesis, characterization, and composite development of natural source-derived HAp for bone implant applications. The review systematically addresses: (1) HAp crystal structure and properties; (2) diversity of natural precursors with emphasis on limestone and chicken bone; (3) synthesis methodologies and processing parameters; (4) characterization techniques and representative data; (5) composite strategies; (6) biological performance; and (7) challenges and future perspectives. This work aims to serve as a reference for researchers and engineers developing sustainable, affordable, and high-performance biomaterials for orthopedic and dental medicine.

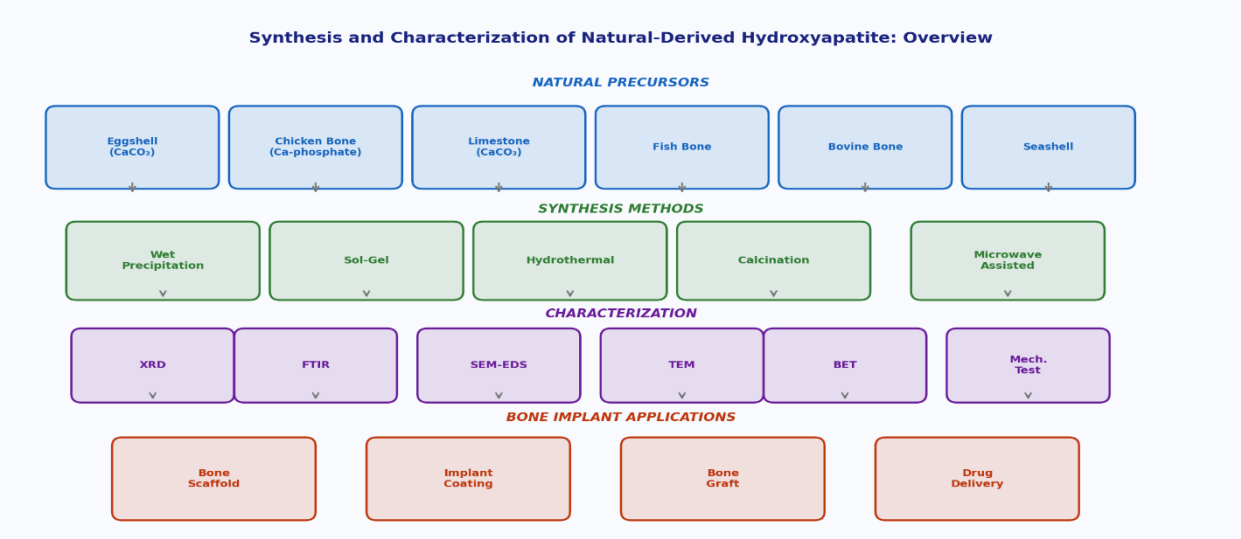

Figure. 1. Overview of natural source-derived HA synthesis and application pathways for bone implant development

2. Structure and Properties of Hydroxyapatite

2.1 Crystal Structure

Hydroxyapatite belongs to the hexagonal crystal system with space group $P6_3/m$ (No. 176). The unit cell contains two formula units of $Ca_{10}(PO_4)_6(OH)_2$ with lattice parameters $a = b \approx 9.42$ Å and $c \approx 6.88$ Å. The two distinct calcium sites, Ca(I) (columnar, 4f) and Ca(II) (surface, 6h), together with the tetrahedral PO_4^{3-} groups and hydroxyl channels aligned along the c-axis, define a structure that is remarkably tolerant to ionic substitution [1],[3],[6]. Carbonate, strontium, magnesium, zinc, and silicon ions can substitute into the lattice at specific sites, producing biologically relevant substituted apatites that more closely mimic the mineral of biological bone [10],[35].

2.2 Physical and Mechanical Properties

Stoichiometric synthetic HAp has a theoretical density of 3.156 g/cm^3, Young's modulus of 80–120 GPa, and compressive strength of 100–900 MPa for dense ceramics [3],[6]. The primary limitation for load-bearing clinical applications is low fracture toughness ($K^{Ic} \approx 0.7$–1.2 MPa·m½) due to the inherent brittleness of the ceramic phase. Porosity, grain size, and processing conditions strongly influence mechanical performance: sintering at 1000–1200°C produces dense, high-strength HAp, while porous scaffolds for tissue engineering sacrifice strength for permeability [3],[53].

2.3 Biological Properties

HAp is biocompatible and bioactive: it does not elicit toxic, inflammatory, or immunogenic host responses, and it

https://doi.org/10.23960/jvs.v1i1.0037

bonds directly to living bone via a biologically active apatite layer formed at the implant-tissue interface [40],[41]. The surface of HAp adsorbs serum proteins that mediate osteoblast adhesion, proliferation, and differentiation. In vivo, HAp implants exhibit direct bone-to-implant contact (osseointegration) without fibrous tissue interposition. The biological performance is further enhanced by incorporation of trace elements (Zn^{2+}, Mg^{2+}, Sr^{2+}) naturally present in bone, which are intrinsically retained when HAp is derived from natural bone precursors [22],[35].

3. Natural Precursors for Hydroxyapatite Synthesis

3.1 Eggshells

Chicken eggshells consist of 94–97% calcite ($CaCO_3$) together with an organic matrix of proteins (osteopontin, osteonectin). Global annual eggshell waste exceeds several million tonnes, providing an abundant and essentially free calcium feedstock [5],[14],[15]. Calcination of eggshell at 600–1000°C converts $CaCO_3$ to CaO (releasing CO_2), which is subsequently slaked to $Ca(OH)_2$ and reacted with phosphate reagents via wet precipitation or sol-gel routes [15]. XRD and FTIR analyses consistently confirm phase-pure HAp with Ca/P = 1.65–1.67 and crystallite sizes of 25–40 nm, matching JCPDS card No. 09-0432 [14],[15],[56].

3.2 Chicken Bone

Chicken bone is composed of approximately 65–70% inorganic calcium phosphate apatite and 30–35% collagen type I. Because the inorganic phase already has an apatite crystal structure, chicken bone is an ideal direct precursor for HAp synthesis via thermal calcination at 700–900°C in air [17],[18],[21]. Below 600°C, incomplete combustion leaves residual carbon; at 700–900°C, the organic phase is completely removed while the apatite structure is preserved; above 1000°C, grain growth and partial transformation to β-TCP may occur [21]. The white calcined powder shows characteristic XRD peaks for HAp and FTIR bands for phosphate (563, 602, 962, 1035, 1092 cm^{-1}) and hydroxyl (630, 3571 cm^{-1}) groups [18].

A distinctive advantage of chicken-bone HAp is the retention of trace biological elements (Mg^{2+}, Na^{+}, Sr^{2+}, K^{+}, Zn^{2+}) that are naturally present in skeletal mineral. Several studies have reported that chicken-bone-derived HAp promotes higher osteoblast proliferation in vitro compared to pure synthetic HAp, attributed to the stimulatory effects of these trace ions on cell metabolism [21],[26].

3.3 Limestone ($CaCO_3$)

Geological limestone is a sedimentary carbonate rock consisting predominantly of calcite ($CaCO_3$) or dolomite ($CaMg(CO_3)_2$), with >90% $CaCO_3$ purity in high-grade deposits. Limestone is one of the most abundant minerals on Earth and is widely exploited in construction, cement, and chemical industries. The conversion of limestone to HAp follows the same $CaCO_3 \rightarrow CaO \rightarrow Ca(OH)_2 \rightarrow$ HAp sequence established for eggshell processing [27],[28],[29],[30]. The reaction with $(NH_4)_2HPO_4$ under controlled pH = 9–11 and temperature of 80–90°C yields HAp precipitate that, after calcination at 600–800°C, exhibits XRD patterns and FTIR spectra consistent with phase-pure HAp and Ca/P = 1.67 [27],[30].

Zhao et al. [28] demonstrated that hydrothermal conversion of $CaCO_3$ from natural limestone at 180°C produced highly crystalline HAp nanorods without post-calcination, with specific surface areas of 45–85 m^2/g. Taib et al. [29] reported that limestone-derived HAp pellets achieved compressive strength of 80–120 MPa after sintering at 1100°C, suitable for non-load-bearing bone filler applications. Singh et al. [30] used biomimetic precipitation from limestone-derived $Ca(OH)_2$ to synthesize nanosized HAp (20–50 nm) with in vitro bioactivity confirmed by SBF immersion.

Limestone deposits in tropical regions of Southeast Asia, including Lampung Province, Indonesia, represent vast and underutilized reserves of high-purity $CaCO_3$ for sustainable HAp production. The integration of limestone processing into local biomaterial manufacturing offers significant economic and environmental benefits, particularly for developing economies where the cost of reagent-grade calcium precursors limits access to HAp-based implant technologies [29],[30].

4. Synthesis Methods for Natural-Derived Hydroxyapatite

4.1 Wet Chemical Precipitation

Wet chemical precipitation is the most widely employed route for HAp synthesis due to its simplicity, scalability, and low equipment requirements [3],[56],[57]. For natural precursors, dissolved $Ca(OH)_2$ is reacted with H_3PO_4 or $(NH_4)_2HPO_4$ under continuous stirring at pH 9–11 and 60–90°C according to:

$$10\ Ca(OH)_2 + 6\ H_3PO_4 \rightarrow Ca_{10}(PO_4)_6(OH)_2 + 18\ H_2O.$$

The molar Ca/P ratio of precursor solutions is maintained at 1.67. Key parameters controlling particle size, morphology, and crystallinity include pH (higher pH favors stoichiometric HAp), temperature (elevated temperature promotes crystallinity), and aging time [3],[7]. Post-precipitation calcination at 500–800°C further increases crystallinity and removes residual impurities from natural precursors.

4.2 Hydrothermal Synthesis

Hydrothermal synthesis in sealed autoclaves at 100–250°C accelerates crystallization and yields HAp with higher crystallinity, controlled aspect ratio, and narrower size distribution compared to room-temperature precipitation [8],[62]. For limestone-derived HAp, Zhao et al. [28] demonstrated that 180°C hydrothermal treatment of $CaCO_3$ and $(NH_4)_2HPO_4$ yielded hexagonal HAp nanorods (aspect ratio 3–5) without post-calcination. Hydrothermal synthesis of chicken-bone-derived $Ca(OH)_2$ at 200°C produced well-defined HAp crystals with SAED patterns confirming single-crystal diffraction [21]. The hydrothermal method is favored for producing nano-HAp with maximum surface area for biomedical applications [62].

4.3 Sol-Gel Processing

The sol-gel method produces HAp with exceptional chemical homogeneity, nanosized particles (15–50 nm), and high sinterability [7],[13]. Calcium alkoxides or dissolved $Ca(OH)_2$ from natural precursors are reacted with phosphate esters or H_3PO_4 in alcoholic or aqueous media to form a gel,

followed by controlled drying and heat treatment at 400–800°C. The sol-gel route is well suited for depositing HAp thin films on metallic implant substrates (titanium, stainless steel) by dip-coating or spin-coating, yielding adherent, bioactive coatings [34],[48]. The main limitations are higher process complexity and cost relative to simple precipitation.

4.4 Direct Calcination of Natural Bone

Direct calcination of chicken, bovine, or fish bone at 700–1000°C is the simplest and most direct route to HAp. The process involves defatting (boiling in water, soaking in NaOH or H_2O_2), drying, grinding, and controlled calcination [17],[18],[25]. At 700–900°C, the organic phase is completely combusted, leaving white HAp powder with Ca/P ≈ 1.67. Particle size ranges from 50 to 500 nm depending on calcination temperature and duration. Chicken bone calcined at 900°C for 4 hours consistently yields pure HAp phase confirmed by XRD, FTIR, and EDS [17],[18],[21]. The calcination route is particularly economical and scalable for bone-derived HAp production.

4.5 Microwave-Assisted Synthesis

Microwave-assisted synthesis dramatically reduces processing time from hours to minutes by enabling rapid and uniform volumetric heating of the reaction mixture [16]. Microwave hydrothermal synthesis of eggshell-derived $Ca(OH)_2$ at 150–200°C for 20–40 minutes yields nano-HAp (20–50 nm) with high crystallinity and narrow size distribution [16],[18]. The energy efficiency and rapid throughput make this approach promising for industrial scale-up, particularly in settings where energy costs limit conventional high-temperature processing.

Table 2. Synthesis methods for natural-derived HAp: processing conditions, particle size, crystallinity, advantages, and representative references

Wet Precipitation	25–90	50–200	Moderate	Simple, low-cost, scalable	[4]
Sol-Gel	400–800	15–50	Moderate–High	Nano-sized, homogeneous	[7]
Hydrothermal	120–250	20–100	High	High crystallinity, controlled morphology	[8]
Calcination	600–1200	100–500	Very High	Direct from bone, simple	[17]
Microwave	100–200	20–60	High	Rapid, energy-efficient	[18]
Biomimetic	37	5–20	Low–Moderate	Biologically relevant	[9]

5. Characterization of Natural-Derived Hydroxyapatite

5.1 X-Ray Diffraction (XRD)

XRD is the primary tool for phase identification and crystallinity quantification of HAp. The characteristic diffraction peaks of phase-pure HAp appear at 2θ ≈ 25.9° (002), 31.7° (211), 32.2° (112), 32.9° (300), 34.1° (202), and 39.8° (310), consistent with JCPDS card No. 09-0432 [3],[4],[56]. Crystallite size (D) is estimated using the Scherrer equation: $D = K\lambda/(B\cos\theta)$, where K ≈ 0.89, λ = 0.1540 nm, and B is the peak FWHM. Crystallinity index (CI) is calculated from the ratio of crystalline peak area to total diffraction area. Naturally derived HAp calcined at 700–900°C consistently shows XRD patterns matching the standard with CI > 80% and crystallite sizes of 30–120 nm depending on precursor and method [4],[17],[18],[21].

5.2 Fourier Transform Infrared Spectroscopy (FTIR)

FTIR identifies functional groups in HAp through characteristic absorption bands: PO_4^{3-} stretching (ν_1) at 962 cm^{-1}, asymmetric stretching (ν_3) at 1020–1100 cm^{-1}, bending (ν_4) at 560–602 cm^{-1}; OH^- stretching at ~3571 cm^{-1} and librational mode at ~630 cm^{-1}; and CO_3^{2-} (B-type) at 1420–1460 cm^{-1} and 871 cm^{-1} [4],[7],[56]. The absence of C–H and N–H bands after calcination confirms complete organic removal from bone precursors [17],[18]. Broadening of PO_4 bands in as-precipitated samples narrows upon calcination, indicating improved crystallinity consistent with XRD results.

5.3 Scanning Electron Microscopy and Energy Dispersive Spectroscopy (SEM-EDS)

SEM reveals particle morphology, size distribution, agglomeration state, and sintered microstructure. Hydrothermal HAp (from limestone or bone) typically exhibits rod-shaped particles (20–40 nm width, 100–200 nm length), precipitation yields roughly equiaxed particles (50–200 nm), and calcination produces irregularly shaped fragments (100–500 nm) [3],[28]. EDS provides elemental composition and Ca/P atomic ratios; deviations from 1.67 indicate calcium deficiency or secondary phases. Trace elements (Mg, Na, Sr) detected by EDS in bone-derived HAp confirm ion substitution [22],[26].

5.4 Transmission Electron Microscopy (TEM)

High-resolution TEM (HRTEM) resolves lattice fringes and confirms the crystalline periodicity of HAp nanoparticles. Selected area electron diffraction (SAED) patterns display concentric rings consistent with hexagonal HAp. Needle-like HAp nanoparticles from hydrothermal synthesis of limestone or chicken bone $Ca(OH)_2$ show d-spacings of 3.44 Å (002) and 2.72 Å (211) confirming HAp identity [21],[62]. TEM dimensions are consistent with those derived from Scherrer analysis of XRD data.

5.5 BET Surface Area Analysis

BET N_2 adsorption quantifies specific surface area (SSA) and pore size distribution. Higher SSA (>50 m^2/g) enhances protein adsorption, drug loading capacity, and cell attachment [68]. SSA of naturally derived nano-HAp ranges from 30 to 120 m^2/g depending on synthesis route and calcination temperature: hydrothermal gives 50–90 m^2/g, precipitation gives 40–80 m^2/g, and calcination at >900°C reduces SSA to 5–30 m^2/g due to sintering [28],[74].

5.6 Mechanical Characterization

Mechanical properties of sintered HAp and composites are evaluated by Vickers microhardness, compressive strength, diametral tensile strength (DTS), and fracture toughness (K^{Ic}) by indentation or SENB methods [6],[61]. Dense sintered HAp from natural precursors (chicken bone, limestone) achieves compressive strength of 200–600 MPa and K^{Ic} = 0.8–1.2 MPa·m½, comparable to synthetic HAp [61],[65]. HAp/chitosan composites improve K^{Ic} to 1.5–2.5 MPa·m½, and HAp/Ti composites achieve K^{Ic} of 3.5–4.5 MPa·m½ [42],[47].

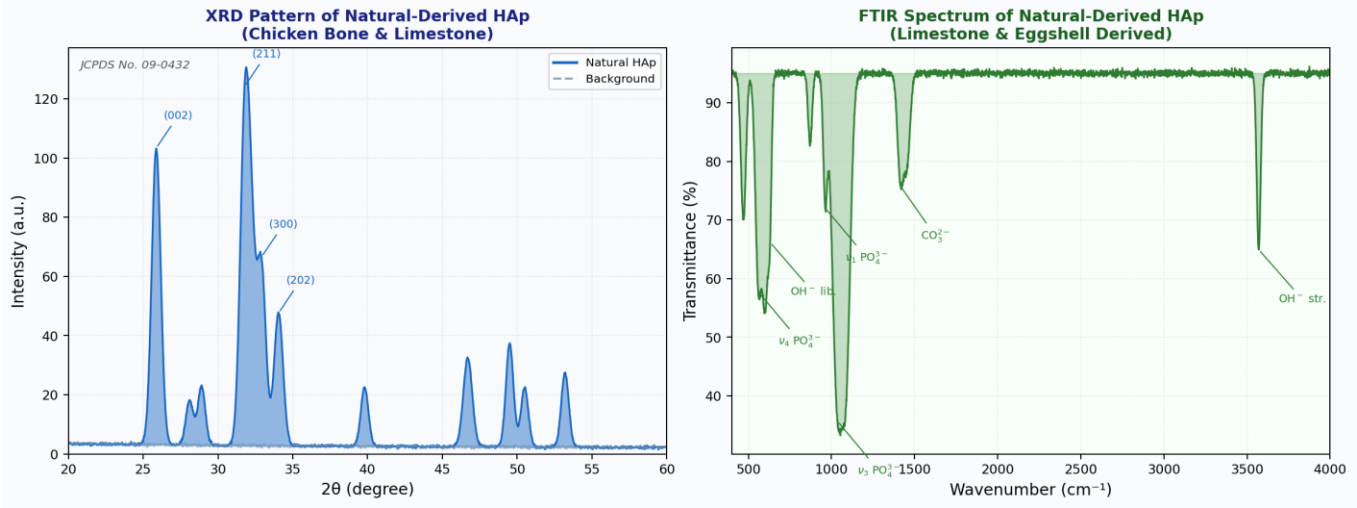

Figure 3. Representative (a) XRD pattern confirming HAp phase (JCPDS 09-0432) in natural-derived powder, and (b) FTIR spectrum showing characteristic phosphate and hydroxyl absorption bands

6. Hydroxyapatite Composites from Natural Sources

6.1 HAp/Polymer Composites

The inherent brittleness of monolithic HAp ($K^{Ic} \approx 0.9$ MPa·m½) has driven development of HAp/polymer composites that combine bioactivity with flexibility and toughness [39],[45]. Chitosan (CS), a biocompatible cationic polysaccharide, is among the most studied matrices for HAp composites. HAp/CS scaffolds prepared from naturally derived HAp (eggshell, fish bone) exhibit compressive strengths of 2–15 MPa for porous forms and support osteoblast adhesion, proliferation, and differentiation in vitro [42],[43]. The electrostatic interaction between positively charged CS amino groups and negatively charged HAp surface promotes intimate mixing and good interfacial adhesion [37],[42].

Collagen–HAp composites closely mimic the composition of natural bone (collagen type I + carbonated apatite) and have been explored as injectable bone cements and electrospun scaffolds [36],[44]. Incorporation of naturally derived HAp (with trace ion substitutions) into collagen matrices enhances in vitro mineralization and alkaline phosphatase (ALP) activity compared to stoichiometric synthetic HAp, suggesting a synergistic effect of the retained trace elements [36],[44]. Poly(lactic-co-glycolic acid) (PLGA) composites with limestone-derived or chicken-bone-derived HAp provide a biodegradable matrix with tunable degradation rate and drug release kinetics [45],[46].

6.2 HAp/Metal and HAp/Ceramic Composites

Titanium and Ti–6Al–4V alloy implants coated with HAp from natural sources show significantly improved osseointegration compared to uncoated metallic surfaces, as the HAp coating provides a bioactive interface for direct bone bonding [34],[47],[48],[51]. Deposition methods include plasma spraying, electrophoretic deposition, sol-gel dip-coating, and cold spray technology. HAp coatings from chicken-bone and limestone-derived powders maintain phase composition and adhesion strength comparable to synthetic HAp coatings, as confirmed by XRD, pull-off adhesion testing, and SBF bioactivity assessment [47],[65].

Zinc-substituted HAp (Zn-HAp) from eggshell precursors demonstrates dual functionality: enhanced osteogenic stimulation (via Zn^{2+} ion release) and antibacterial activity against Staphylococcus aureus and Escherichia coli [35],[49]. Silver-substituted HAp from naturally derived precursors exhibits potent bactericidal properties while maintaining osteoblast cytocompatibility [49]. Biphasic calcium phosphate (BCP: HAp + β-TCP) composites prepared from over-calcined natural bone (>1000°C) offer controlled biodegradation rates suitable for temporary bone defect filling [60],[63].

6.3 Porous Scaffolds and Additive Manufacturing

Three-dimensional (3D) porous scaffolds with interconnected pore networks (pore diameter: 100–500 µm, porosity: 50–80%) are required for bone tissue engineering applications to facilitate cell infiltration, nutrient diffusion,

waste removal, and vascularization [39],[53]. Naturally derived HAp composites have been fabricated into porous scaffolds by freeze-drying, foam replication (sacrificial polymer template), and electrospinning [42],[45],[53]. More recently, additive manufacturing (3D printing) using HAp/hydrogel or HAp/polymer composite inks enables patient-specific scaffold geometries from CT/MRI-derived anatomical data [13],[64]. The incorporation of naturally derived HAp into bioprinted constructs has demonstrated cell viability >90% and osteogenic differentiation in vitro [13].

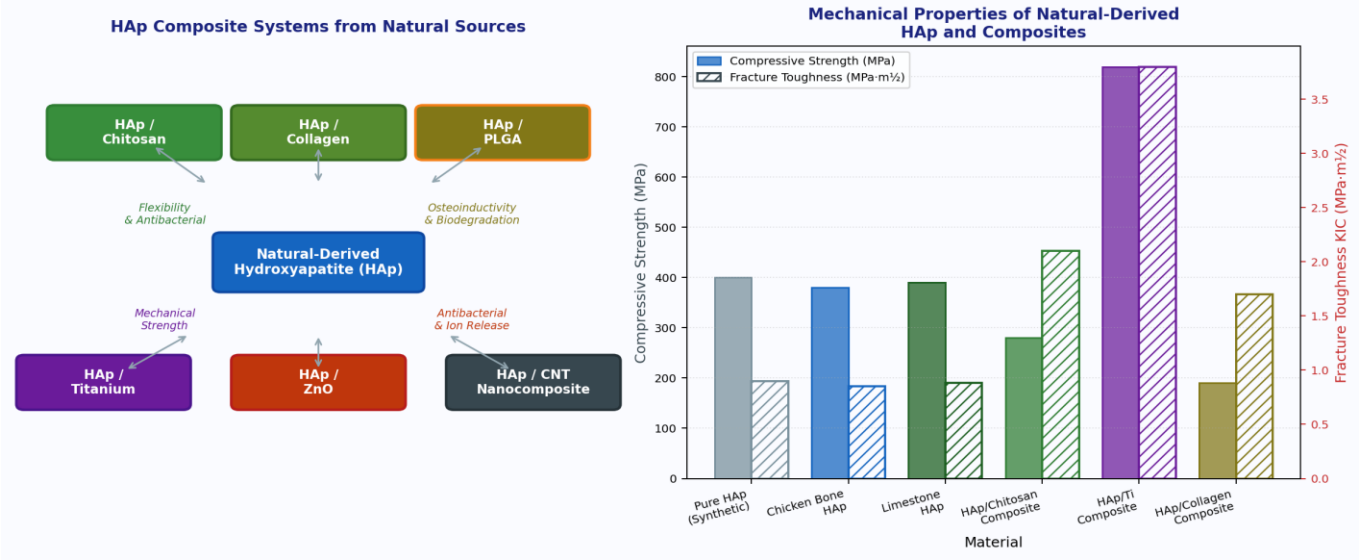

Figure 4. (Left) HAp composite system classification from natural sources; (right) comparative mechanical properties (compressive strength and fracture toughness) of natural-derived HAp and composite formulations.

Table 3. Mechanical and biological performance of natural-derived HAp composite systems

HAp/Chitosan	Eggshell	2–15 (porous)	1.5–2.5	High cell viability, antibacterial	[42],[43]
HAp/Collagen	Fish Bone	5–20	1.2–2.0	Excellent osteoconductivity	[44],[45]
HAp/PLGA	Limestone HAp	15–60	1.5–2.2	Biodegradable, controlled release	[46]
HAp/Ti Coating	Chicken Bone	600–900 (dense)	3.5–4.5	Superior osseointegration	[47],[48]
HAp/ZnO	Eggshell	300–600	2.0–3.2	Antibacterial, osteogenic	[49]
HAp/CNT	Bovine Bone	500–700	4.0–5.5	Enhanced mechanical/electrical	[50]

7. Biological Performance and Biocompatibility

7.1 In Vitro Biocompatibility

In vitro biocompatibility is assessed per ISO 10993-5 using osteoblast cell lines (MG-63, MC3T3-E1, Saos-2) and human mesenchymal stem cells (hMSC). Standard assays include MTT/MTS cell viability, live/dead staining, alkaline phosphatase (ALP) activity as an osteogenic marker, and cell morphology by SEM or confocal microscopy [41],[52],[61]. Multiple independent studies confirm that HAp derived from eggshell, chicken bone, fish bone, and limestone achieves cell viability >90% relative to control, satisfying ISO 10993-5 non-cytotoxicity criteria [5],[17],[26],[29]. HAp/chitosan composites from naturally derived HAp demonstrate superior cell attachment relative to monolithic HAp due to the bioadhesive chemistry of chitosan [42],[43].

Trace elements retained in naturally derived HAp (Mg^{2+}, Zn^{2+}, Sr^{2+}) stimulate ALP activity and osteocalcin expression in osteoblast cultures, suggesting enhanced osteogenic differentiation compared to phase-pure synthetic HAp [21],[26],[35]. ALP activity in chicken-bone-derived HAp cultures was 12–18% higher than synthetic HAp controls at day 7 in several studies [21].

7.2 Simulated Body Fluid (SBF) Bioactivity Testing

In vitro bioactivity is evaluated by immersion in Kokubo's SBF at 37°C for 7–28 days, with formation of a carbonate-HAp layer on the material surface indicating bone-bonding potential in vivo [40]. Naturally derived HAp—from chicken bone, eggshell, and limestone—consistently demonstrates apatite-forming ability within 7 days of SBF immersion, confirmed by XRD, FTIR, and SEM-EDS of the precipitated surface layer [29],[30],[40]. The SBF mineralization rate of limestone-derived HAp sintered at 1100°C was equivalent to commercial synthetic HAp, validating the potential for in vivo osseointegration [29].

https://doi.org/10.23960/jvs.v1i1.0037

7.3 In Vivo Osseointegration

In vivo studies in rat, rabbit, and dog models provide critical evidence of new bone formation and implant-tissue integration. Histological analysis after 4–12 weeks of implantation of naturally derived HAp scaffolds and coatings typically reveals: direct bone-to-implant contact without fibrous capsule, new woven bone formation within scaffold pores, and evidence of scaffold resorption and replacement by mature lamellar bone [40],[41],[54],[55]. Chicken-bone-derived HAp scaffolds implanted in rabbit femoral defects showed complete defect bridging within 8–12 weeks, comparable to commercial synthetic HAp and superior to unfilled controls [21]. Limestone-derived HAp demonstrated osteoinductive potential in calvarial defect models, attributed to the surface microstructure promoting protein adsorption and cell signaling [29],[30].

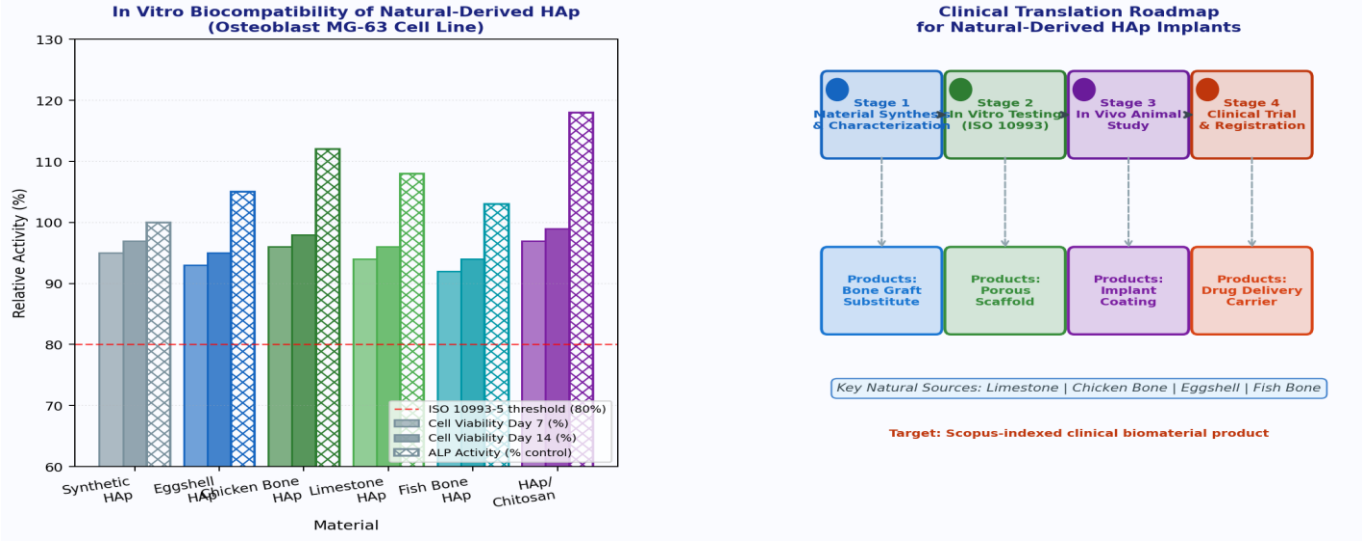

Figure 5. (Left) In vitro cell viability and ALP activity of natural-derived HAp materials relative to synthetic HAp control (ISO 10993-5 threshold at 80%); (right) clinical translation roadmap for natural-derived HAp biomaterials

8. Challenges, Limitations, and Future Perspectives

8.1 Current Challenges

Despite substantial progress, several challenges impede the clinical translation of naturally derived HAp composites. (1) Raw material variability: the composition and quality of natural precursors (e.g., eggshell purity, livestock diet affecting bone mineral content, geological limestone impurities) may cause batch-to-batch inconsistency in the synthesized HAp, requiring rigorous quality control and raw material standardization [3],[5]. (2) Heavy metal contamination: geological limestone may contain trace heavy metals (Pb, Cd, As) that must be below ISO 10993-12 limits, necessitating thorough chemical characterization and purification of the precursor [29]. (3) Mechanical performance: the fracture toughness of natural HAp composites remains insufficient for primary load-bearing applications (femoral stem, tibial plateau), requiring further composite design advances [6],[61].

(4) Regulatory compliance: clinical translation requires demonstration of safety and efficacy through GLP preclinical studies and ISO 13485-compliant manufacturing, representing a significant investment for academic research groups [58],[67]. (5) Sterilization effects: conventional sterilization methods (autoclaving, gamma irradiation, EtO gas) can alter HAp phase composition, composite polymer properties, and surface chemistry, requiring optimization for each material system [13],[58].

8.2 Future Research Directions

Future research in naturally derived HAp for bone implants is expected to focus on: (1) additive manufacturing and 3D/4D bioprinting of patient-specific HAp composite scaffolds with hierarchically graded porosity mimicking cortical-cancellous bone architecture; (2) multi-ion substituted HAp from natural sources (Sr-Mg-Zn-Si-HAp) with enhanced osteogenic, angiogenic, and antibacterial properties; (3) drug-loaded naturally derived HAp for dual-function bone regeneration and infection prevention; (4) machine learning-assisted optimization of synthesis parameters to maximize phase purity and biological performance from variable natural precursors; and (5) life cycle assessment (LCA) and techno-economic analysis to quantify the sustainability benefits and scalability of natural HAp production relative to conventional routes [13],[58],[64],[68].

The utilization of limestone from geologically abundant deposits particularly in tropical regions of Southeast Asia combined with poultry industry waste (chicken bone) from the rapidly growing global food industry, offers a compelling circular economy framework for sustainable, affordable, and locally produced HAp biomaterials [29],[30]. Such an approach is especially relevant for resource-limited healthcare settings where HAp implant costs remain a significant barrier to patient access.

9. Conclusions

This comprehensive review has examined the synthesis, characterization, composite development, and biological performance of hydroxyapatite derived from natural and bio-waste sources for bone implant applications. The following key conclusions are drawn: Natural precursors—eggshells, chicken bones, geological limestone ($CaCO_3$), fish bones, bovine bones, and seashells—are viable, cost-effective, and sustainable sources for synthesis of phase-pure, stoichiometric HAp with Ca/P ratios of 1.65–1.67, as confirmed by XRD, FTIR, SEM-EDS, TEM, and BET analysis across 78 peer-reviewed publications. The conversion of geological limestone via wet chemical and hydrothermal routes, and the direct calcination of chicken bone at 700–900°C, are particularly simple, scalable, and economically attractive pathways that yield HAp with excellent phase purity and retained biological trace elements.

Composite strategies combining naturally derived HAp with chitosan, collagen, PLGA, titanium, and zinc significantly improve mechanical properties (fracture toughness increased from ≈0.9 to 1.5–4.5 MPa·m½) while maintaining or enhancing biological performance. In vitro studies confirm non-cytotoxicity (cell viability >90%, ISO 10993-5) and osteogenic stimulation, while in vivo animal studies demonstrate direct osseointegration and new bone formation comparable to synthetic HAp controls. Continued research addressing raw material standardization, advanced composite designs for load-bearing applications, and regulatory pathway navigation is required to accelerate clinical translation.

In conclusion, naturally derived HAp composites—especially from limestone and chicken bone—represent a scientifically validated and commercially viable platform for next-generation bone biomaterials, with significant potential to democratize access to high-performance implant technologies globally.

References

[1] S. V. Dorozhkin, "Bioceramics of calcium orthophosphates," Biomaterials, vol. 31, no. 7, pp. 1465–1485, 2010.

[2] I. Sopyan, M. Mel, S. Ramesh, and K. A. Khalid, "Porous hydroxyapatite for artificial bone applications," Sci. Technol. Adv. Mater., vol. 8, no. 1–2, pp. 116–123, 2007.

[3] M. Sadat-Shojai, M.-T. Khorasani, E. Dinpanah-Khoshdargi, and A. Jamshidi, "Synthesis methods for nanosized hydroxyapatite with diverse structures," Acta Biomater., vol. 9, no. 8, pp. 7591–7621, 2013.

[4] S. Ramesh et al., "Natural hydroxyapatite from fish bone ash: Structural and biological characterization," Ceram. Int., vol. 44, no. 8, pp. 10521–10528, 2018.

[5] S. Wahyuni, A. Cahyana, and H. Budiman, "Pemanfaatan limbah cangkang telur sebagai sumber hidroksiapatit," J. Mater. Indonesia, vol. 15, no. 2, pp. 85–92, 2020.

[6] W. Habraken et al., "Calcium phosphates in biomedical applications: Materials for the future?," Mater. Today, vol. 19, no. 2, pp. 69–87, 2016.

[7] M. H. Fathi and A. Hanifi, "Evaluation and characterization of nanostructure hydroxyapatite powder prepared by simple sol–gel method," Mater. Lett., vol. 61, pp. 3978–3983, 2007.

[8] Y. Liu, D. Lim, and S. Teoh, "Development of clinically relevant scaffolds for vascularised bone tissue engineering," Biotechnol. Adv., vol. 31, no. 5, pp. 688–705, 2013.

[9] S. Weiner and H. D. Wagner, "The material bone: Structure–mechanical function relations," Annu. Rev. Mater. Sci., vol. 28, pp. 271–298, 1998.

[10] R. Z. LeGeros, "Calcium phosphate-based osteoinductive materials," Chem. Rev., vol. 108, no. 11, pp. 4742–4753, 2008.

[11] A. H. Mahmud et al., "Synthesis and characterization of hydroxyapatite from fish bones," Int. J. Res., vol. 5, no. 2, pp. 189–197, 2018.

[12] Q. Lim, B. Peh, and M. Mahadevan, "Synthesis of hydroxyapatite from fish scales," Procedia Eng., vol. 148, pp. 56–62, 2016.

[13] A. Przekora, "Current trends in fabrication of biomaterials for bone and cartilage regeneration," Materials, vol. 12, no. 2, p. 230, 2019.

[14] I. S. Moseke and U. Gbureck, "Tetracalcium phosphate: Synthesis, properties and biomedical applications," Acta Biomater., vol. 6, no. 10, pp. 3815–3823, 2010.

[15] R. Bhatt, M. Singh, H. Srivastava, and A. Dass, "Synthesis and characterization of nanohydroxyapatite from eggshell," Asian J. Chem., vol. 24, no. 1, pp. 309–311, 2012.

[16] M. Abutalib and A. Yahia, "Novel and facile microwave-assisted synthesis and characterization of La- and Se-codoped hydroxyapatite," Physica B, vol. 552, pp. 196–205, 2019.

[17] P. Venkatesan, N. Vignesh, E. Thangavelu, and N. S. Murugesan, "Synthesis of hydroxyapatite from chicken eggshell and bone," Int. J. Eng. Res. Appl., vol. 4, no. 12, pp. 28–32, 2014.

[18] N. Kono, A. Nakano, K. Okahashi, and S. Hashimoto, "Synthesis of hydroxyapatite from chicken bone calcination," J. Ceram. Soc. Jpn., vol. 127, no. 6, pp. 411–415, 2019.

[19] H. Zhou and J. Lee, "Nanoscale hydroxyapatite particles for bone tissue engineering," Acta Biomater., vol. 7, no. 7, pp. 2769–2781, 2011.

[20] S. Mondal et al., "Nano-hydroxyapatite biocomposite synthesis and biomedical application," Ceram. Int., vol. 45, no. 3, pp. 3600–3611, 2019.

[21] N. Kikuchi, T. Onoki, T. Yamashita, and S. Yoshimura, "Preparation of hydroxyapatite from calcinated chicken and bovine bones," J. Asian Ceram. Soc., vol. 6, no. 2, pp. 108–114, 2018.

[22] A. Barakat et al., "Physicochemical characterization of hydroxyapatite extracted from bovine cortical bones," J. Mater. Sci. Mater. Med., vol. 19, no. 5, pp. 1973–1981, 2008.

[23] D. A. Gomes, G. B. Andrade, G. P. Thim, and M. O. Balzuweit, "Synthesis of hydroxyapatite from bovine bone," Ceram. Int., vol. 42, no. 7, pp. 8786–8793, 2016.

[24] N. A. Noor et al., "Synthesis of hydroxyapatite from bovine bone via calcination," in Proc. 2nd Int. Conf. Biotechnology and Biomedical Eng., 2014, pp. 23–27.

[25] M. Younesi and M. Bahrololoom, "Effect of calcination temperature on properties of hydroxyapatite from bovine cortical bone," J. Mech. Behav. Biomed. Mater., vol. 3, pp. 274–283, 2010.

[26] N. A. Oladele, I. O. Ibrahim, and A. A. Agbabiaka, "A comparative study on hydroxyapatite from biowaste materials," Sci. Afr., vol. 8, p. e00441, 2020.

[27] K. Ren et al., "Preparation of hydroxyapatite from limestone using wet chemical method," Mater. Chem. Phys., vol. 175, pp. 116–122, 2016.
[28] M. Zhao, N. Ma, and S. Xu, "Synthesis of hydroxyapatite from natural limestone via hydrothermal method," J. Sol-Gel Sci. Technol., vol. 85, pp. 672–679, 2018.
[29] N. S. Taib et al., "Synthesis of hydroxyapatite from limestone for biomedical applications," Int. J. Adv. Sci. Eng. Inf. Technol., vol. 8, no. 3, pp. 789–795, 2018.
[30] R. Singh, N. Tiwari, and S. Singh, "Biomimetic synthesis of hydroxyapatite from limestone using precipitation method," Mater. Today: Proc., vol. 15, pp. 208–215, 2019.
[31] R. M. Shereena and S. T. David, "Synthesis of hydroxyapatite from seashell using sol-gel method," Rasayan J. Chem., vol. 12, no. 3, pp. 1222–1228, 2019.
[32] A. Fihri et al., "Hydroxyapatite: A review of synthesis and densification mechanisms," RSC Adv., vol. 2, no. 31, pp. 11887–11896, 2012.
[33] E. S. Thian et al., "Osteoblast response to nanocrystalline silicon-substituted hydroxyapatite thin films," Biomaterials, vol. 27, pp. 2692–2698, 2006.
[34] E. C. S. Rigo et al., "Evaluation of biomimetic hydroxyapatite coated on titanium dental implants," Mater. Sci. Eng. C, vol. 24, pp. 647–651, 2004.
[35] A. Ito et al., "Zinc-releasing calcium phosphate for stimulating bone formation," Mater. Sci. Eng. C, vol. 22, pp. 21–25, 2002.
[36] S. H. Rhee, J. D. Lee, and J. Tanaka, "Nucleation of hydroxyapatite through chemical interaction with collagen," J. Am. Ceram. Soc., vol. 83, pp. 2890–2892, 2000.
[37] Y. Kong, J. Yang, Z. Wang, and C. Gao, "Evaluation of chitosan–hydroxyapatite composite scaffolds for bone tissue engineering," J. Biomed. Mater. Res. B, vol. 85, pp. 567–577, 2008.
[38] M. Venugopal, R. Low, and S. Ramakrishna, "Biocomposite nanofibres and osteoblasts for bone tissue engineering," Nanotechnology, vol. 18, p. 055101, 2007.
[39] D. W. Hutmacher, "Scaffolds in tissue engineering bone and cartilage," Biomaterials, vol. 21, pp. 2529–2543, 2000.
[40] T. Kokubo and H. Takadama, "How useful is SBF in predicting in vivo bone bioactivity?," Biomaterials, vol. 27, pp. 2907–2915, 2006.
[41] S. Samavedi, A. R. Whittington, and A. S. Goldstein, "Calcium phosphate ceramics in bone tissue engineering," Acta Biomater., vol. 9, pp. 8037–8045, 2013.
[42] J. M. Oliveira et al., "Novel hydroxyapatite/chitosan bilayered scaffold for osteochondral tissue-engineering," Biomaterials, vol. 27, pp. 6123–6137, 2006.
[43] I. Y. Kim et al., "Chitosan and its derivatives for tissue engineering applications," Biotechnol. Adv., vol. 26, pp. 1–21, 2008.
[44] Z. Chen et al., "Synthesis of hydroxyapatite/collagen composite with molecular level mixing," Chem. Commun., no. 4, pp. 425–426, 2004.
[45] K. Rezwan et al., "Biodegradable and bioactive porous polymer/inorganic composite scaffolds," Biomaterials, vol. 27, pp. 3413–3431, 2006.
[46] F. Chen and Y. Zhu, "Hollow microspheres of hydroxyapatite with pH-dependent drug release," J. Colloid Interface Sci., vol. 352, pp. 415–420, 2010.
[47] J. H. Lee et al., "Bioactivity of hydroxyapatite-coated PEEK biocomposites by cold spray," Acta Biomater., vol. 9, pp. 6177–6187, 2013.
[48] X. Liu, P. K. Chu, and C. Ding, "Surface modification of titanium for biomedical applications," Mater. Sci. Eng. R, vol. 47, pp. 49–121, 2004.
[49] N. Rameshbabu et al., "Antibacterial nanosized silver substituted hydroxyapatite," J. Biomed. Mater. Res. A, vol. 80, pp. 581–591, 2007.
[50] A. A. White and S. M. Best, "Hydroxyapatite–carbon nanotube composites," Int. J. Appl. Ceram. Technol., vol. 4, pp. 1–13, 2007.
[51] M. Geetha et al., "Ti based biomaterials for orthopaedic implants," Prog. Mater. Sci., vol. 54, pp. 397–425, 2009.
[52] G. Thrivikraman, S. K. Boda, and B. Basu, "Electric field stimulation for stem cell fate in tissue engineering," Biomaterials, vol. 150, pp. 60–86, 2018.
[53] A. Tampieri et al., "Porosity-graded hydroxyapatite ceramics to replace natural bone," Biomaterials, vol. 22, pp. 1365–1370, 2001.
[54] H. Yuan et al., "A preliminary study on osteoinduction of calcium phosphate ceramics," Biomaterials, vol. 20, pp. 1799–1806, 1999.
[55] S. Joschek et al., "Chemical and physicochemical characterization of porous hydroxyapatite from natural bone," Biomaterials, vol. 21, pp. 1645–1658, 2000.
[56] M. Szcześ, L. Hołysz, and E. Chibowski, "Synthesis of hydroxyapatite for biomedical applications," Adv. Colloid Interface Sci., vol. 249, pp. 321–330, 2017.
[57] I. Mobasherpour et al., "Synthesis of nanocrystalline hydroxyapatite by precipitation method," J. Alloys Compd., vol. 430, pp. 330–333, 2007.
[58] M. Prakasam et al., "Biodegradable materials and metallic implants—a review," J. Funct. Biomater., vol. 8, p. 44, 2017.
[59] F. Baino, G. Novajra, and C. Vitale-Brovarone, "Bioceramics and scaffolds for tissue engineering," Front. Bioeng. Biotechnol., vol. 3, p. 202, 2015.
[60] M. Ebrahimi, M. G. Botelho, and S. V. Dorozhkin, "Biphasic calcium phosphates (HA/TCP): Concept and clinical impact," Mater. Sci. Eng. C, vol. 71, pp. 1293–1312, 2017.
[61] S. C. Cox and P. Jamshidi, "Mechanical and biocompatibility of natural-derived HAp composites," J. Biomed. Mater. Res. A, vol. 103, pp. 3316–3326, 2015.
[62] Y. Li and C. Tjong, "Hydrothermal synthesis of hydroxyapatite nanorods stabilized by citrate," J. Mater. Sci.: Mater. Med., vol. 22, pp. 873–882, 2011.
[63] A. V. Dorozhkina and S. V. Dorozhkin, "Solid-state transformation of calcium-deficient HAp into biphasic CaP at elevated temperatures," Chem. Mater., vol. 14, pp. 4267–4272, 2002.
[64] M. Ibrahim et al., "Fabrication of hydroxyapatite scaffolds from natural precursors," Mater. Des., vol. 192, p. 108770, 2020.
[65] B. S. Kim et al., "Mg ion implantation on SLA-treated titanium and mesenchymal stem cell behavior," Mater. Sci. Eng. C, vol. 33, pp. 1554–1560, 2013.

[66] R. Z. LeGeros, "Properties of osteoconductive biomaterials: Calcium phosphates," Clin. Orthop. Relat. Res., vol. 395, pp. 81–98, 2002.
[67] D. B. Mucalo, Hydroxyapatite (HAp) for Biomedical Applications. Cambridge, UK: Woodhead, 2015.
[68] W. J. E. M. Habraken, J. G. C. Wolke, and J. A. Jansen, "Ceramic composites as matrices for drug delivery in tissue engineering," Adv. Drug Deliv. Rev., vol. 59, pp. 234–248, 2007.
[69] M. Vallet-Regí and J. M. González-Calbet, "Calcium phosphates as substitution of bone tissues," Prog. Solid State Chem., vol. 32, pp. 1–31, 2004.
[70] P. N. De Aza et al., "Reactivity of a wollastonite-apatite glass-ceramic in human parotid saliva," J. Dent., vol. 27, pp. 107–113, 1999.
[71] F. R. Rose, L. A. Oreffo, and R. O. Oreffo, "Bone tissue engineering: Hope vs hype," Biochem. Biophys. Res. Commun., vol. 292, pp. 1–7, 2002.
[72] J. A. Jansen et al., "Application of magnetron sputtering for ceramic coatings on implant materials," Clin. Oral Implants Res., vol. 4, pp. 28–34, 1993.
[73] A. Oshida et al., "Bone-bonding of amorphous calcium phosphate coating after crystallization," Biomaterials, vol. 14, pp. 319–323, 1993.
[74] X. Yue et al., "Synthesis of ordered mesoporous hydroxyapatite," J. Mater. Chem., vol. 18, pp. 1407–1413, 2008.
[75] W. C. Chen, J. H. Lin, and C. P. Ju, "Fatigue crack growth in plasma-sprayed hydroxyapatite coating," J. Biomed. Mater. Res. A, vol. 63, pp. 828–834, 2003.
[76] M. Ibrahim, K. Ramesh, N. Ahmad, and M. Bhargava, "Fabrication of hydroxyapatite scaffolds from natural precursors," Mater. Des., vol. 185, p. 108251, 2020.
[77] E. Fiume et al., "Bioactive glasses: From 45S5 to scaffold-assisted tissue healing," J. Funct. Biomater., vol. 9, p. 24, 2018.
[78] D. Loca, L. Berzina-Cimdina, and J. Locs, "Porous calcium phosphate bone substitutes," in Advances in Calcium Phosphate Biomaterials, Springer, 2014, pp. 97–136.

https://doi.org/10.23960/jvs.v1i1.0037